Biosensors and Bioelectronics 140 (2019) 111329

Contents lists available at ScienceDirect

Biosensors and Bioelectronics

journal homepage: www.elsevier.com/locate/bios

A novel lab-on-chip platform enabling axotomy and neuromodulation in a multi-nodal network

Rosanne van de Wijdeven[a], Ola Huse Ramstad[b], Vibeke Devold Valderhaug[b], Peter Köllensperger[c], Axel Sandvig[d], Ioanna Sandvig[b], Øyvind Halaas[a,*]

[a] Department of Clinical and Molecular Medicine, Faculty of Medicine and Health Sciences, Norwegian University of Science and Technology (NTNU), PO Box 8905 MTFS, NO-7491, Trondheim, Norway
[b] Department of Neuromedicine and Movement Science, Faculty of Medicine and Health Sciences, Norwegian University of Science and Technology (NTNU), N-7491, Trondheim, Norway
[c] NTNU NanoLab, 7049, Trondheim, Norway
[d] Department of Neurology, St Olav´s Hospital, 7030, Trondheim, Norway

ARTICLE INFO

Keywords:
Microfluidic chip
Micro-electrode array
Synaptic connectivity
Functional connectivity
Plasticity
Axotomy

ABSTRACT

Lab-on-chip platforms, such as microfluidic chips and micro-electrode arrays (MEAs) are powerful tools that allow us to manipulate and study neurons in vitro. Microfluidic chips provide a controlled extracellular environment that structures neural networks and facilitates isolation and manipulation at a sub-cellular level. Furthermore, MEAs enable measurement of extracellular electrophysiological activity from single neurons to entire networks. Here, we demonstrate the design, fabrication and application of a 3-nodal microfluidic chip integrated with MEAs as a versatile study platform for neurobiology and pathophysiology. In this work, we evaluate the use of the microfluidic chip to structure a neural network into three separate nodes, interconnected through tunnels that isolate and guide axons into a channel, thus facilitating synaptic contacts between neurons originating from opposite nodes. Furthermore, we demonstrate the utility of the MEA for monitoring developing activity and intra-/inter nodal connectivity of the structured neural network. Finally, we demonstrate the versatility of the platform in two separate experiments. First, we demonstrate the ability to measure intra- and inter-nodal dynamic responses to a fluidically isolated chemical stimulation. Then, we demonstrate the feature of the microfluidic chip enabling the disruption of functional connectivity between nodes and examination of the immediate activity response of the neural network. The platform enables in vitro modelling of neural networks to study their functional connectomes in the context of neurodegenerative disease and CNS trauma, including spinal cord injury.

1. Introduction

The complexity of the central nervous system confounds efforts in elucidating the intrinsic repair mechanisms of the central nervous system (CNS) in response to neurodegenerative disease or trauma. This knowledge is vital for developing therapeutic interventions that stimulate and/or enhance repair. Micro-engineered platforms, such as microfluidic chips, offer a reductionist in vitro approach in combination with high spatiotemporal control of both cells and their chemical environment. In the last two decades, a number of microfluidic chips have emerged that are specifically designed to compartmentalize subpopulations of neurons into nodes and isolate axons from their somata via structurally guided axon growth into microsized tunnels that interconnect the nodes. Such microfluidic chips have been used as a platform to study fundamental neurobiology mechanisms such as axon outgrowth and neural network formation (Park et al., 2006; Tsantoulas et al., 2013; Coquinco et al., 2014; van de Wijdeven et al., 2018) as well as impairment of neural networks related to disease or injury (Lei et al., 2016; Wang et al., 2017).

Several studies have successfully demonstrated the integration of microelectrode arrays (MEAs) within such microfluidic chips, enabling the measurement of extracellular electrophysiological activity from a structured neural network (Morin et al., 2006; Kanagasabapathi et al., 2011; Forró et al., 2018). Furthermore, the separation of somata and axonal segments allows targeted manipulation (Pan et al., 2015) and recording. A study by A. Gladkov et al. (2017), confirmed unidirectional axon growth, through specially designed directional microtunnels, demonstrating unidirectional spike propagation captured with

* Corresponding author.
E-mail addresses: rwijdeven@gmail.com (R. van de Wijdeven), oyvind.halaas@ntnu.no (Ø. Halaas).

https://doi.org/10.1016/j.bios.2019.111329
Received 19 March 2019; Received in revised form 13 May 2019; Accepted 15 May 2019
Available online 23 May 2019
0956-5663/

an integrated MEA (Gladkov et al., 2017). R. Habibey et al., (2017), combined a two-compartment design microfluidic chip with an MEA to study both morphology and activity of pure axonal branches within the axon tunnels (Habibey et al., 2017). Additionally, the amplification effect the tunnels have on axonal signals enables extraction of the weaker amplitude signals (Dworak and Wheeler, 2009). Signal recording and signal quality are closely related to the distance between the signal source and the electrode. Therefore, confining the neural network on top of the electrodes increases the likelihood of electrodes recording neuronal activity (Toivanen et al., 2017). However, most studies using such an integrated system adjust the design of the microfluidic chip to the layout of commercially available MEAs (Multi Channel Systems), which poses limitations to the microfluidic chip design and, by the same token, also confounds signal resolution.

In this study, we demonstrate the design, fabrication and application of a 3-nodal microfluidic chip integrated with an MEA. The addition of a third cell compartment affords additional complexity in the neural networks (Poli et al., 2015). Our microfluidic chip consists of open cell compartments, also referred to as nodes, interconnected with microtunnels and an incorporated synaptic channel perpendicular to the tunnels (Kilinc et al., 2011; Tong et al., 2015; Virlogeux et al., 2018). The design of the 3-nodal microfluidic chip thus provides access not only to the neuronal somata in the open cell compartments, but also to a dense area of isolated axons and synaptic connections, as demonstrated by A. Virlogeux et al. (2018). The MEA layout is custom-designed to align with the features of the 3-nodal microfluidic chip. The layout of the electrodes was designed to record activity from the subpopulation of neurons within each node, as well as from the isolated neurites in the synaptic channel and the tunnels that interconnect opposite nodes. We demonstrate the functional development of structured co-cultures of cortical neurons and astrocytes over 18 days resulting in functional inter-nodal connectivity. In addition, as a proof-of-principle, we chemically manipulated neuronal activity in nodes and measured the response in activity within the targeted node as well as the intra-nodal response. Furthermore, we show the utility of the synaptic channel as a method to reproducibly axotomize axons, as was originally demonstrated by Z. Tong et al. (2015). The integrated electrodes enable quantitative measurement of the effect of axotomy at the site of the injury as well as its inter-nodal effect. The platform presented here is thus a well-suited tool to model aspects of neurodegenerative disease pathology in terms of synaptic connectivity and synaptic plasticity, and also to study the effects of axotomy on neural networks. Moreover, this versatile platform can be used in studies investigating therapeutic interventions aimed at promoting CNS repair.

2. Material and methods

2.1. Microfluidic chip fabrication

The microfluidic chips were fabricated using photoresist moulds that were made with standard lithography techniques. Details of the fabrication can be found in our recent publication (van de Wijdeven et al., 2018). The polydimethylsiloxane (PDMS) microfluidic chips were cured for 4 h at 65 °C. The nodes (Ø 4 mm) as well as the inlets and outlets (Ø 2 mm), were punched open with a punching device (Fig. 2A). PDMS debris from the punching process was removed with scotch tape and afterwards the chips were rinsed consecutively in acetone, ethanol (70%) and deionised water. The microfluidic chips were irreversibly bonded to either glass coverslips or MEAs. The alignment of chips onto the MEA will be described in more detail in section 2.2.1. From now on, we refer to the microfluidic chips bonded on top of the MEAs as 'structured MEAs'.

2.2. Structured MEA fabrication

The MEAs were fabricated using 4-inch borosillicate glass wafers (V015.04–1011, Plan Optik), with a 1 mm thickness, as the substrate material. The cleaning process of wafers consisted of consecutive washes in acetone and isopropanol and, after drying under nitrogen gas, the substrates were treated with oxygen plasma (80 sccm, 0.34 mbar, 80 W) for 5 min. After a short dehydration bake, the substrates were spin-coated with a 4 μm thick layer of photoresist (maN 440, micro resist technology GmbH) (Fig. 1 I). The MEA design was created with Clewin software (WieWeb software, Enschede) and transferred to a masklessaligner (MLA150, Heidelberg). The masklessaligner then transferred the pattern of the MEA circuit into the film, using a 402 nm laser (2000 mJ/cm^2). An undercut was created to facilitate lift-off in a later process step, by developing the exposed structures for 2.30 min (ma-D332/S Microchem) (Fig. 1 II). Prior to metal evaporation, the substrate was descummed for 1 min. The metallization of the circuit was conducted with e-beam evaporation (ATC-2200V, AJA inc.). First, a 50 nm thick adhesion layer of titanium was evaporated, followed by a 100 nm thick layer of Platinum (Pt) (Fig. 1 III). A lift-off in acetone removed the remaining photoresist and the metal on top, leaving only the metal circuit adhered to the glass on the substrate. After descumming for 1 min, a 450 nm thick layer of silicon nitride (Si_3N_4) was deposited onto the entire substrate by means of plasma enhanced vapour deposition at a moderate temperature of 300 °C (PLasmaLab System 100-PECVD, Oxford Instruments) (Fig. 1.IV). Prior to coating with resist, the substrate was treated with an O_2 plasma for 1 min to decrease the hydrophobicity of the surface to improve the spin-coating procedure. The spin-coating of a new photoresist layer (maN 440), exposure and development were done in accordance to previously stated steps. The developed film was used as an etch mask in the subsequent step (Fig. 1 V). The Si_3N_4 film on top of the electrodes and contact points for the data-acquisition recording system, was dry etched in an inductively coupled plasma with various fluorocarbon gases (CHF_3, CF_4, 0_2) (Plasmalab System 100 ICP-RIE 180, Oxford Instruments), guided by the etch mask until the metal surface was reached (Fig. 1 VI). The MEAs were diced with a saw (DAD323, DISCO) in squares of 48 × 48 mm out of the glass wafer. Finally, the photoresist etch mask was removed with acetone (Fig. 1 VII).

2.2.1. Microfluidic chip alignment on MEAs

Prior to alignment, the surfaces of the microfluidic chips (pattern upwards) and MEAs were treated with oxygen plasma (80 sccm, 0.34 mbar, 80 W, 1 min). A drop of ethanol (70%) was placed in between to aid alignment under a microscope. The bonding was finalized by heating the structured MEAs on a hotplate (75 °C), until the ethanol was evaporated, while applying moderate pressure. After several washes in deionised (DI) Type 1 water to remove any remnants of ethanol, the microfluidic chip was filled with DI water and stored at 4 °C.

2.3. Microfluidic chip preparation

The preparation steps for cell seeding of the microfluidic chip bonded to glass coverslips and of the structured MEAs were identical. Prior to coating, all devices were sterilized under UV light for 1 h. All devices were coated with Poly-D-Lysine (4.5 μg/cm^2) (P6407, Sigma Aldrich) for 1 h at RT and washed three times in phosphate buffered saline (PBS). Poly-D-Lysine promotes cell adhesion and was applied in accordance with the cortical neuron protocol (MAN0001574). Next, the devices were incubated with Laminin (15 μg/ml) (Natural mouse Laminin, Thermo Fisher), which was diluted in Leibovitz-15 (1X) medium and supplemented with Sodium Bicarbonate (40X), overnight at RT. The following day, Laminin was replaced with Neuronal growth media and the devices were incubated at 37 °C for 2hr prior to cell seeding. The neuronal media consisted of Neural basal (1X), FBS (20X), PenStrep (100X), B27 (50X) and GlutaMAX (100X).

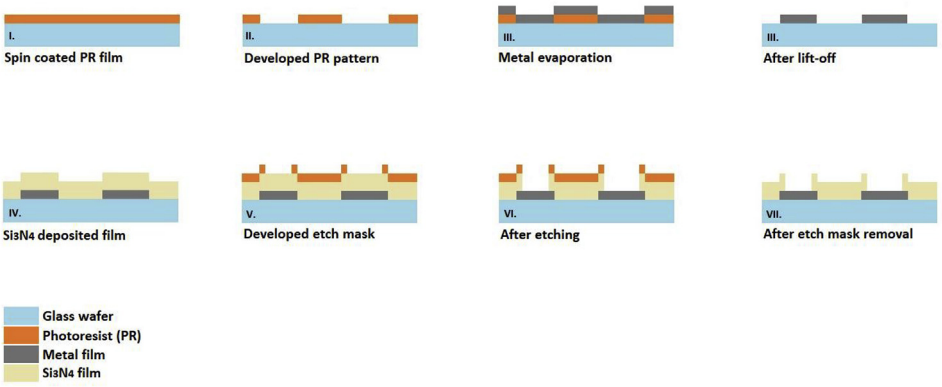

Fig. 1. Schematic overview of MEA fabrication steps: (I.) A photoresist (PR) film is spin coated on top of wafer; (II.) After exposure and development, the PR pattern is established; (III.) A thin film metal layer of titanium and platinum is evaporated onto the PR pattern; (III.) After lift-off in acetone the PR is removed along with the metal on top; (IV.) A passivation layer of silicon nitride (Si_3N_4) is deposited; (V.) A new PR pattern that serves as an etch mask is developed; (VI.) After etching, the Si3N4 is removed from the surface of the metal electrodes; (VII.) The PR etch mask is removed and the MEA fabrication is complete. (For interpretation of the references to colour in this figure legend, the reader is referred to the Web version of this article.)

2.4. Cell seeding and maintenance

A feeder layer of Rat Primary Cortical Astrocytes (P7, N7745-100, Thermo Fisher) was seeded in each cell compartment (3000 cells/compartment) two days in advance of seeding Rat Primary Cortical Neurons (A10840-01, Thermo Fisher). Two days later, cortical neurons were seeded on top of the feeder layer (0 Days In Chip = 0 DIC). Cell thawing as well as seeding was done mostly in accordance with the Gibco protocol (MAN0001574). However, in order to obtain a high concentration of cells in a small volume, the cell suspension (3.5 mL) had to be centrifuged at a low rotation speed (20 RPM, 2 min). Additionally, cells were thawed in neuronal growth media supplemented with Rock inhibitor (Y-27632; Sigma Aldrich) (100X). The primary cortical neurons were seeded (30,000–35,000 cells/compartment) by adding 40 μL of cell suspension to each cell compartment. Two thirds of neuronal growth media were replenished every third day. At 14 DIC, the microfluidic chips bonded on top of coverslips were fixed for immunocytochemistry. The cell cultures within the structured MEAs were maintained till 27 DIC.

2.5. Immunocytochemistry and imaging

The fixation and immunocytochemistry procedure for the cells in the microfluidic chips were described in detail in a previous study (van de Wijdeven et al., 2018). Primary antibodies were purchased from Abcam and secondary antibodies from Thermo Fisher, unless stated otherwise. The cells were fixed in the microfluidic chips using paraformaldehyde (PFA), first in media (2%) and once more in a fresh PFA solution (4%). Prior to overnight incubation in primary antibody solution, the fixed cells were blocked for 2 h in a solution of PBS, goat serum and Triton-X. Cells were characterized by staining for chicken anti-GFAP (ab4674), mouse anti-MAP2 (13–500, thermos fisher), mouse anti-TUJ-1 (ab18018) and chicken anti-neurofilament heavy (ab4680). To determine synaptic activity, we stained for rabbit anti-CAMKII (ab134041), rabbit anti-Piccolo (abb20664) and mouse anti-PSD-95 (ab13552). The following day, after washing, the secondary antibody solution was applied for 3 h at room temperature. The secondary antibodies used were: Alexa Fluor 350 (goat anti-mouse), Alexa Fluor 488 (goat anti-mouse) Alexa Fluor 488 (goat anti-rabbit), Alexa Fluor 546 (goat anti-chicken). In addition, Hoechst (33258) was used to stain the cell nuclei. Afterwards, the cells were washed with PBS and stored in PBS. Imaging was completed within the next two days. The cells were imaged using a Zeiss LSM 510 Meta Live Confocal microscope, EVOS FL Auto 2 (Invitrogen) and a Zeiss Axio Vert.A1 Microscope. The obtained images were processed in ImageJ (U. S. National Institutes of Health, Bethesda, Maryland, USA).

2.6. Experimental setup of the structured MEA

Impedance of the electrodes for each MEA was measured in PBS prior to coating and seeding, using an impedance testing device (MEA-IT60, Multichannel Systems). The average impedance of the electrodes was 142 kΩ with a standard deviation of 16 kΩ. MEA recordings were made using the MEA2100 workstation (Multi Channel Systems) at a sampling rate of 10,000 Hz. Each recording lasted between 5 and 10 min. During each recording, the temperature was kept at 37 °C using a temperature controller (TC01, MCS). A gas permeable membrane constructed onto a 3D printed (Ultimaker 2) cap was placed over the structured MEAs during recordings to maintain sterility, while also allowing gas exchange and minimizing evaporation from the media.

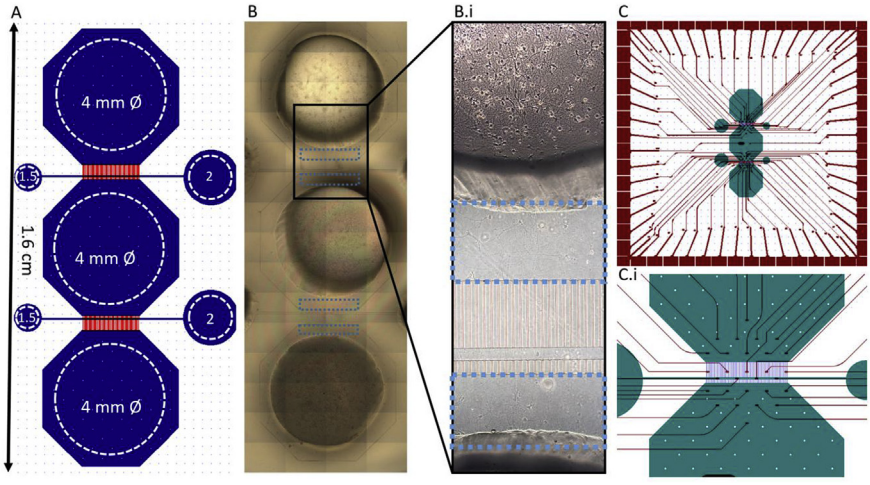

Fig. 2. Overview of 3-nodal microfluidic chip design and MEA layout. A) Design of microfluidic chip (Clewin). White perforated line marks punched-out areas. B) Tiled brightfield images of all cell compartments of the chip. Active zones marked in blue. B.i) Stitched phase contrast image of active zones between two nodes. C) Design of MEA layout aligned with the 3-nodal chip design (Clewin). C.i) Magnified image of inter-nodal area (Clewin). (For interpretation of the references to colour in this figure legend, the reader is referred to the Web version of this article.)

2.6.1. Measurement of the functional development of the structured neural network

Measurements of the extracellular activity of the neural networks that were cultured on the structured MEA were conducted at 7, 14, and 18 DIC across four structured MEAs. Media changes, when necessary, were done after a measurement so as not to disturb the extracellular ion balance. Functional development was determined using the spike rate within each of the nodes of the structured MEAs, which is discussed in more detail in section 2.7. Furthermore, the recordings were analysed for bursting activity, which was first observed at 14 DIC for all of the structured MEAs.

2.6.2. Compartment specific neurotransmitter stimulation

As a proof of concept, cells on the structured MEA were chemically modulated with neurotransmitters. Prior to adding the neurotransmitter, a 5-min baseline measurement was obtained. The neurotransmitter was added to one of the compartments and one of the synaptic channels (supplementary material. Fig. E). Two types of neurotransmitters were used; the inhibitory γ-Aminobutyric acid (GABA) (100 μM) and excitatory N-methyl-d-aspartic acid (NMDA) (25 μM). The compartment was fluidically isolated by applying hydrostatic pressure, so that no diffusion of the neurotransmitter towards opposite direction could occur (supplementary materials Fig. A). The neurotransmitter was added within 5 μl of neuronal growth media. This was necessary to prevent inadvertent change in activity as a result of a complete media change. A 10-min recording was conducted directly after applying the neurotransmitter solution.

2.6.3. Axotomy

The synaptic channels incorporated in the three-nodal microfluidic chip also enable transection of axons and dendrites that are growing through the tunnels (Tong et al., 2015). As a proof of concept, one of the structured MEAs was used as a platform to study the post-axotomy response of the disconnected neural networks. First, a baseline (pre-axotomy) recording was obtained. The axotomy was performed using a pipette to introduce an air bubble into the synaptic channel, which propagated from the inlet to the outlet (supplementary material. Fig. F). After introducing two of these propagating air-bubbles, most axons in the synaptic channel were severed. Post-axotomy, the media in the synaptic chamber were replenished and a recording was subsequently performed.

2.7. MEA data analysis

In brief, MEA data processing proceeded as follows. Raw data captured using Multichannel systems Experimenter software were filtered off-line in Neuroexplorer (5th ed, Nex Technologies) using a 4th order Butterworth bandpass filter of 300–3000 Hz. Spike detection on the filtered data was achieved using the standard bidirectional thresholding method in Neuroexplorer, with amplitudes exceeding 4 standard deviations from the electrode mean marked as spikes. Spike timings were binned at 100 ms for functional connectivity analysis, and 1 s bins for spike analysis. Functional development of the neural network was determined by averaging the spike rate data of all electrodes within each node for each measurement (7, 14 and 18 DIC). Binned spike timings were exported to MATLAB (2018, Mathworks) for functional connectivity analysis and visualisation. Functional connectivity was determined by concurrent spike timings as assessed by Pearson's correlation coefficient. The functional connectivity was plotted using Okomarov/schemaball (MATLAB central File Exchange, Komarov, Oleg, retrieved 2017.01.15).

3. Results and discussion

3.1. Design and application of the 3-nodal microfluidic chip and structured MEA

Key features of the design of the 3-nodal microfluidic chip are based on existing designs previously demonstrated among others by Z. Tong et al. (2015) and A. Virlogeux (2018) as well as our 4-nodal and 6-nodal microfluidic chip as described in an earlier study (van de Wijdeven et al., 2018). Three octagonal shaped nodes (Ø 5 mm), also referred to as cell compartments, are connected by 52 microtunnels of 10 μm in width, 5 μm in height and 500 μm in length. The cell compartments are almost completely open, and thus easily accessible, except for the area in front of the microtunnels, which we also refer to as the active area (Fig. 2A, B, B i). A channel of 50 μm in width and 45 μm in height intersects the microchannels at a distance of about 100 μm from the central node. This design feature enables the observation of synaptic contacts formed by outgrowing axons from opposite nodes (Virlogeux et al., 2018), while it also facilitates axotomy by air bubble formation and propagation within this channel (Tong et al., 2015). This synaptic/axotomy channel is accessible through an inlet and outlet channel.

The electrode layout and dimensions are designed with the objective of obtaining information from neuronal subpopulations rather than single neurons. Of special interest was the ability to record inter-as well as intra-nodal neuronal structural connectivity and functional communication. The microelectrode array consists of 59 recording electrodes and one internal reference electrode, while the layout and contact points for the data-acquisition are compatible with a commercially available recording system (MEA2100 workstation, Multichannel systems). The electrodes have a surface area of 2532 μm^2 and the minimum inter-electrode distance is 300 μm. The electrodes are designed to align with the 3-nodal microfluidic chip; 10 electrodes are located in the centre and active zone of each node, while the middle node has one additional electrode in the centre. For each internodal area, five electrodes are placed underneath the microtunnels and four electrodes are placed in the synaptic channel (Fig. 2C, C.i). The location of the electrodes enables recording of extracellular action potentials (EAPs) from neurons in the centre of each node as well as from neurons and axon bundles between nodes (supplementary material. Fig. B).

3.2. Axon ingrowth and fasciculation through the synaptic channel

To better approximate key functional and structural features of *in vivo* neural networks in our in vitro paradigm, astrocytes and primary cortical neurons were co-cultured in each node. Both the microfluidic chips on top of glass coverslips as well as the structured MEAs contained similar co-cultures (Fig. 3A and B). In addition, using astrocytes as a feeder layer provides neuronal support increasing the probability for a viable long-term culture (> 21DIC) of primary cortical neurons (Potter and DeMarse, 2001). Axon outgrowth towards the tunnels occurred within the first three days after seeding the primary cortical neurons. The first axons reaching adjacent nodes were observed around 7 DIC. From 7 to 14 DIC, increased axon growth into the tunnels and fasciculation of axons were observed in the synaptic channel (Fig. 3C). The synaptic channel thus serves as a window that allows long-term observation/monitoring of axon projection into and out of the tunnels, which would otherwise require the use of live stains or dyes.

3.3. The synaptic channel can be used to modulate and study synaptic features

The cell cultures in the microfluidic chips were fixed at 14DIC, when internodal connectivity is well established (Pan et al., 2015). To demonstrate synaptic connectivity at this timepoint, we performed immunocytochemistry against CaMKII (Fig. 3D,Di-ii-iii). The CamKII protein has been shown to be associated with several long-term

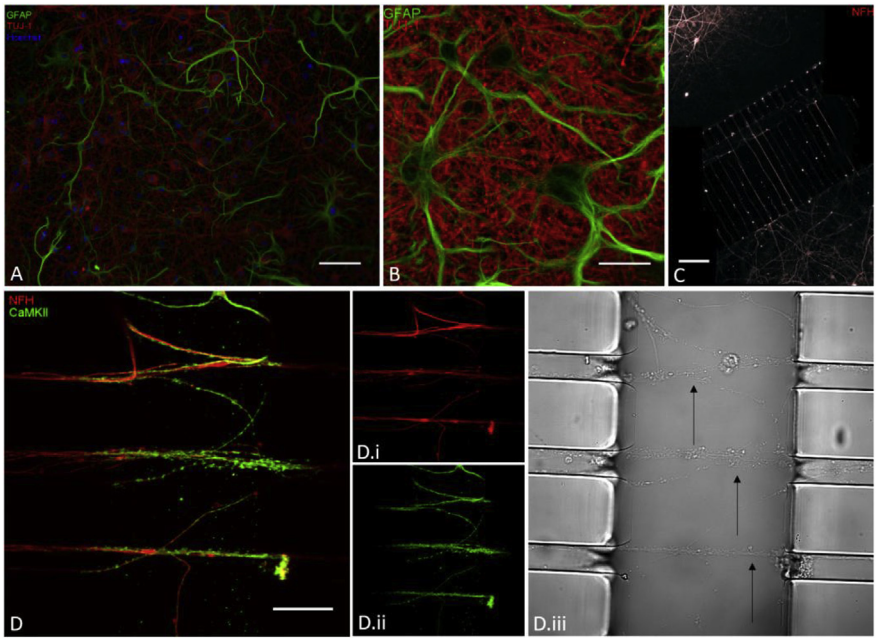

Fig. 3. Immunofluorescence images of the neural network in the microfluidic chips. A) Image shows astrocytes GFAP (green), cortical neurons TUJ-1 (red) and Hoechst (blue) stains the cell nuclei (scale bar 100 μm). B) Magnified image of astrocytes (green) and cortical neurons (red) in a node (scale bar 25 μm). C) Stitched image of neurons and their axons, stained for neurofilament heavy (NFH), showing axonal outgrowth towards the opposite nodes (red) (scale bar 150 μm). D-D.iii) Images demonstrating inter-nodal connectivity, with axons and dendrites in the synaptic channel stained for NFH (red) and CamKII (green) (scale bar 25 μm). (For interpretation of the references to colour in this figure legend, the reader is referred to the Web version of this article.)

potentiation mechanisms (Lisman et al., 2002; Lee et al., 2009; Sanhueza et al., 2011). As was demonstrated in a previous study by Virlogeux et al. (2018), the synaptic channel of the microfluidic chip isolates a dense network of axons and synapses (supplementary material. Fig. C). The volume of the channel is controlled by a separate inlet and outlet, which effectively enables control of the channel's extracellular environment. Therefore, this key feature of the microfluidic chip design facilitates the study of axonal and synaptic plasticity in healthy and perturbed conditions (Taylor et al., 2010).

3.4. Network development and functional interconnectivity between nodes

The functional development of sub-populations of neural networks within each node as well as functional inter-nodal connectivity were determined by analyzing EAP data obtained from the structured MEAs. Recordings were conducted on multiple timepoints. On 7 DIC, mostly random spikes were detected. At 14 DIC, bursting activity was first observed, a common phenomenon for cortical neurons at this timepoint (Pan et al., 2015). By DIC 18, bursting activity was concurrent across nodes (Fig. 4A, supplementary material. Fig. D) with bursts propagating from one node to another through the channels (Fig. 4C, C.i-iiii), and the three nodes were functionally interconnected (Fig. 4B). In addition, overall spiking activity increased from DIC 7 till 18, as can be seen from Fig. 4D (n = 4).

3.5. Intra- and inter-nodal dynamic responses are observed after modulation with neurotransmitters

As a proof of principle demonstrating that the structured MEA can measure dynamic intra- and inter-nodal network responses after manipulation, a chemical neuromodulation experiment was conducted using neurotransmitters. Initially, the intra-nodal dynamics were studied by adding the inhibitor GABA to the central node at 14 DIC. The inhibited node was fluidically isolated from the other nodes by means of hydrostatic pressure (supplementary material. Fig. A). The addition of GABA resulted in a significant decrease of activity within the inhibited node as compared to baseline activity. Additionally, inter-nodal spike propagation was greatly reduced due to the addition of GABA to the central node (Fig. 5A, A.i-ii, C). To further assess the effect of inter-nodal communication, excitatory NMDA was added to an outer node

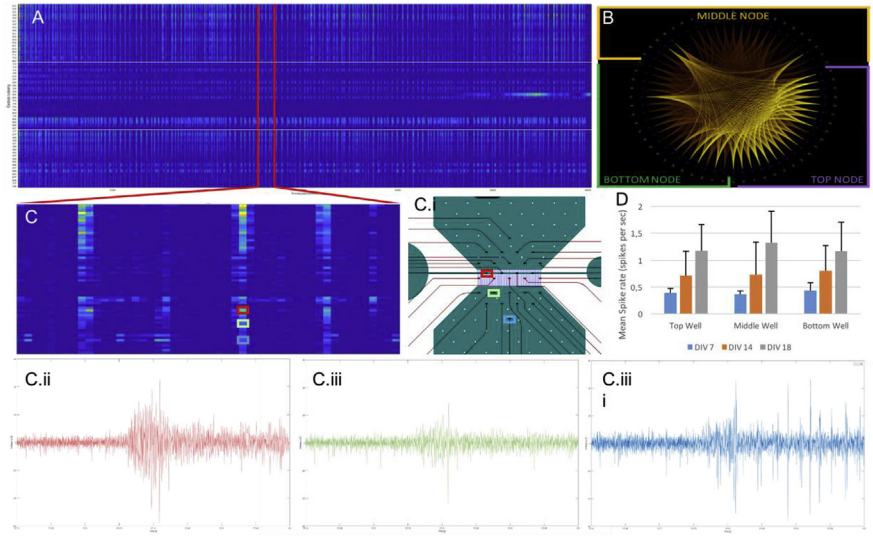

Fig. 4. Analysis of characteristic spiking activity. A) Rasterplot of spiking activity on representative MEA (DIC 18). Note high degree of concurrent spiking (vertical stripes) attributable to internodal bursts. B) Functional map showing connectivity (correlation of concurrent spikes) between electrodes in the 3 nodes at DIC 18. Note the high degree of internodal connectivity (Green: Top node, Purple: Bottom node, Orange: Middle node). C) Rasterplot of 10 s segment, the highlighted electrodes denote the same burst form passing from between electrodes with a millisecond delay. C.i Placement of highlighted electrodes C.ii-iiii) Burst propagation across 3 electrodes from red, green to blue. D) Typical development of spiking activity for each well from DIC 7–18. (For interpretation of the references to colour in this figure legend, the reader is referred to the Web version of this article.)

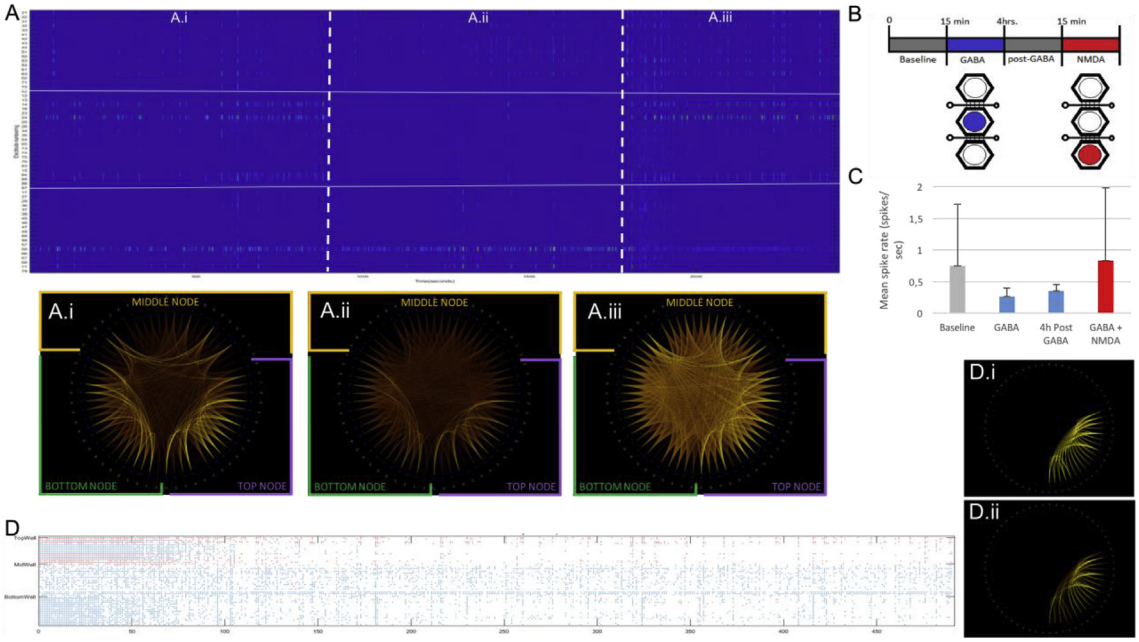

Fig. 5. Activity analysis of chemical modulation A) Rasterplot of spiking activity during chemical stimulation experiment, baseline (left), GABA and 4 h post GABA (middle), NMDA stimulation (right). A.i-iii) Functional connectivity between nodes, baseline (A.i), GABA inhibition (A.ii), NMDA stimulation (A.iii). B) Timeline of neurotransmitter stimulation and recordings, addition of neurotransmitters within the nodes highlighted in blue (GABA) and red (NMDA). C) Mean spike rate in middle chamber during stimulation conditions. Note suppression of activity during GABA addition and disinhibition during NMDA stimulation. The error bars represent the standard deviation of the individual electrodes within the middle node. D) GABA inhibition within the synaptic channel decreases the spike activity in time as demonstrated by the red dots (representing associated electrodes) in the rasterplot. D.i-ii) Functional connectivity between electrodes underneath the axon tunnels and synaptic channel before (D.i) and after (D.ii) GABA inhibition. (For interpretation of the references to colour in this figure legend, the reader is referred to the Web version of this article.)

4 h after addition of GABA (Fig. 5B). The addition of NMDA disinhibited the central node (Fig. 5C) and increased concurrent spiking between all nodes (Fig. 5A iii). To assess the utility of the synaptic channel as a study platform for synapse function and plasticity, we added GABA to a single synaptic channel and directly inhibited synaptic and axonal activity, as was observed by a decrease in the channel's spiking activity and functional connectivity (Fig. 5D.Di-ii). Furthermore, an additional graph demonstrates the increase as well as a decrease in mean spike rate (supplementary material Fig. E). Thus, we could demonstrate that the neural networks in the microfluidic chip represent a functionally interconnected network, which displays dynamic responses to selective manipulation of fluidically isolated nodes in the network. As such, the chip is a powerful tool in the study of adaptive and maladaptive processes in response to disease and damage of the CNS (Fornito et al., 2015).

3.6. The structured MEA enables the study of dynamic responses of a neural network to axotomy

The synaptic channel feature of the microfluidic chip also enables axotomy of isolated axons that interconnect neuronal subpopulations in opposite nodes. Therefore, in this section these channels are referred to as axotomy channels. To do so, an air bubble was created within the axotomy channel by first emptying both inlet and outlet, followed by applying suction at the outlet while simultaneously supplying air to the inlet using pipettes. After two air bubbles passed through the axotomy channel, all axons growing perpendicular to this channel through the tunnels towards opposite nodes were axotomized (Fig. 6A i-ii,C + supplementary material. Fig. F). Functional analysis of pre- and post-axotomy recordings highlights complete abolishment of spiking activity in the affected tunnels, and isolation of the outer node with only intranodal activity remaining (Fig. 6B, B.i). The concept of the axotomy channel has been described in other studies (Kilinc et al., 2011; Tong et al., 2015), however, to our knowledge the combination with an integrated MEA is unique. This design for microfluidic based axotomy, first described by Kilinc et al. (2011) and adapted by Tong et al. (2015) provides a simple structural solution to axotomy compared to elaborate laser or pneumatic based systems (Kim et al., 2009; Hellman et al., 2010; Hosmane et al., 2011; Dollé et al., 2013; Yap et al., 2014; Habibey et al., 2015). While these more advanced systems enable single axon and partial injury assessments, they are ill-suited to network models or high throughput assays. To summarize, our axotomy results demonstrate an additional application of the chip as a platform to study dynamic structural and functional responses of an interconnected neural network to axotomy.

Taken together, the features of this chip design enable manipulation, and selective perturbation of network nodes, hubs and connectivity. Investigation of complex network responses, such as diaschisis or compensation, or key aspects of pathologies, such as spinal cord injury, should be a logical next step when utilizing this platform.

4. Conclusion

In this work, we designed, fabricated and demonstrated the versatility of our 3-nodal microfluidic chip integrated with an MEA. We demonstrate the ability to measure electrophysiological activity related to different stages in the development of the structured neural network. Furthermore, we applied the synaptic/axotomy channel to modulate and perturb isolated cell segments, such as axons, dendrites and synapses. Moreover, we showed the application of the integrated MEA to measure dynamic responses, both intra- and inter-nodal, of the neural network after selective neuromodulation and physical perturbation (i.e. axotomy). In conclusion, the structured MEA is a powerful lab-on-chip platform for the study of fundamental neurobiology and pathophysiology mechanisms. The platform constitutes an advanced tool for studying synaptic plasticity and modelling axotomy, while the

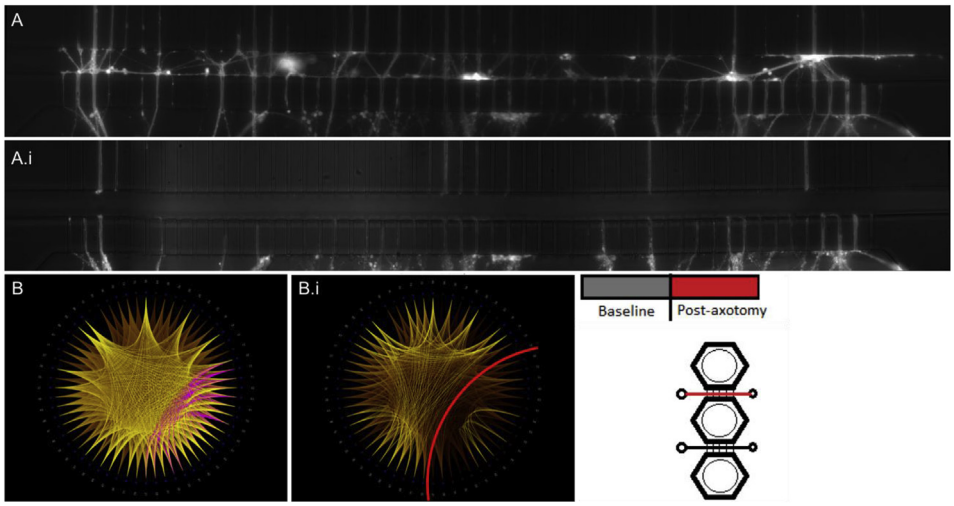

Fig. 6. Fluorescent images and activity analysis of pre- and post-axotomy A. Axonal outgrowth in synaptic channel pre- (A) and post-axotomy (A.i). B. Functional connectivity pre (left, B) and post (right, B.i) axotomy. Affected channel electrodes denoted in purple, red line denotes axotomy location. C. Axotomy location on the microfluidic chip. (For interpretation of the references to colour in this figure legend, the reader is referred to the Web version of this article.)

integrated MEA enables direct quantification of responses from the neural network. Future directions include applying the platform to model pathophysiological aspects of spinal cord injury as well as neurodegenerative diseases, to study acute and chronic dynamic responses in proximally and distally connected nodes of the structured neural network.

Declaration of interest

There are no interests to declare.

Conflict of interest

There are no conflicts to declare.

CRediT authorship contribution statement

Rosanne van de Wijdeven: Conceptualization, Methodology, Writing - original draft, Writing - review & editing. **Ola Huse Ramstad:** Conceptualization, Formal analysis, Software, Writing - original draft, Writing - review & editing. **Vibeke Devold Valderhaug:** Conceptualization, Writing - review & editing. **Peter Köllensperger:** Methodology, Writing - review & editing. **Axel Sandvig:** Supervision, Writing - original draft, Writing - review & editing. **Ioanna Sandvig:** Supervision, Writing - original draft, Writing - review & editing. **Øyvind Halaas:** Supervision, Writing - original draft, Writing - review & editing.

Acknowledgements

This work was supported by the Research Council of Norway, Norwegian Micro- and Nano-Fabrication Facility, NorFab, project number 245963/F50, the NTNU program for Enabling Technologies, (Nanotechnology), and the Liaison Committee between the Central Norway Health Authority and NTNU (Samarbeidsorganet HMN-NTNU). The confocal microscopy was performed at the Cellular and Molecular Imaging Core Facility (CMIC), Norwegian University of Science and Technology (NTNU). CMIC is funded by the Faculty of Medicine at NTNU and Central Norway Regional Health Authority.

Appendix A. Supplementary data

Supplementary data to this article can be found online at https://doi.org/10.1016/j.bios.2019.111329.

References

Coquinco, A., Kojic, L., Wen, W., Wang, Y.T., Jeon, N.L., Milnerwood, A.J., et al., 2014. A microfluidic based in vitro model of synaptic competition. Mol. Cell. Neurosci. 60, 43–52.

Dollé, J.-P., Morrison, B., Schloss, R.R., Yarmush, M.L., 2013. AN ORGANOTYPIC UNIAXIAL STRAIN MODEL USING MICROFLUIDICS. Lab Chip 13 (3). https://doi.org/10.1039/c2lc41063j.

Dworak, B.J., Wheeler, B.C., 2009. Novel MEA platform with PDMS microtunnels enables the detection of action potential propagation from isolated axons in culture. Lab Chip 9 (3), 404–410.

Fornito, A., Zalesky, A., Breakspear, M., 2015. The connectomics of brain disorders. Nat. Rev. Neurosci. 16, 159.

Forró, C., Thompson-Steckel, G., Weaver, S., Weydert, S., Ihle, S., Dermutz, H., et al., 2018. Modular microstructure design to build neuronal networks of defined functional connectivity. Biosens. Bioelectron. 122, 75–87.

Gladkov, A., Pigareva, Y., Kutyina, D., Kolpakov, V., Bukatin, A., Mukhina, I., et al., 2017. Design of cultured neuron networks in vitro with predefined connectivity using asymmetric microfluidic channels. Sci. Rep. 7 (1), 15625.

Habibey, R., Golabchi, A., Latifi, S., Difato, F., Blau, A., 2015. A microchannel device tailored to laser axotomy and long-term microelectrode array electrophysiology of functional regeneration. Lab Chip 15 (24), 4578–4590.

Habibey, R., Latifi, S., Mousavi, H., Pesce, M., Arab-Tehrany, E., Blau, A., 2017. A multielectrode array microchannel platform reveals both transient and slow changes in axonal conduction velocity. Sci. Rep. 7, 8558.

Hellman, A.N., Vahidi, B., Kim, H.J., Mismar, W., Steward, O., Jeon, N.L., et al., 2010. Examination of axonal injury and regeneration in microfluidic neuronal culture using pulsed laser microbeam dissection. Lab Chip 10 (16), 2083–2092.

Hosmane, S., Fournier, A., Wright, R., Rajbhandari, L., Siddique, R., Yang, I.H., et al., 2011. Valve-based microfluidic compression platform: single axon injury and regrowth. Lab Chip 11 (22), 3888–3895.

Kanagasabapathi, T.T., Ciliberti, D., Martinoia, S., Wadman, W.J., Decré, M.M.J., 2011. Dual-compartment neurofluidic system for electrophysiological measurements in physically segregated and functionally connected neuronal cell culture. Front. Neuroeng. 4, 13.

Kilinc, D., Peyrin, J.-M., Soubeyre, V., Magnifico, S., Saias, L., Viovy, J.-L., et al., 2011. Wallerian-like degeneration of central neurons after synchronized and geometrically registered mass axotomy in a three-compartmental microfluidic chip. 19 (1), 149–161.

Kim, Y.-t., Karthikeyan, K., Chirvi, S., Davé, D.P., 2009. Neuro-optical microfluidic platform to study injury and regeneration of single axons. Lab Chip 9 (17), 2576–2581.

Lee, S.-J.R., Escobedo-Lozoya, Y., Szatmari, E.M., Yasuda, R., 2009. Activation of CaMKII in single dendritic spines during long-term potentiation. Nature 458, 299.

Lei, Y., Li, J., Wang, N., Yang, X., Hamada, Y., Li, Q., et al., 2016. An on-chip model for investigating the interaction between neurons and cancer cells. Integrative Biology 8 (3), 359–367.

Lisman, J., Schulman, H., Cline, H., 2002. The molecular basis of CaMKII function in synaptic and behavioural memory. Nat. Rev. Neurosci. 3, 175.

Morin, F., Nishimura, N., Griscom, L., LePioufle, B., Fujita, H., Takamura, Y., et al., 2006. Constraining the connectivity of neuronal networks cultured on microelectrode arrays with microfluidic techniques: a step towards neuron-based functional chips. Biosens. Bioelectron. 21 (7), 1093–1100.

Pan, L., Alagapan, S., Franca, E., Leondopulos, S.S., DeMarse, T.B., Brewer, G.J., et al., 2015. An in Vitro Method to Manipulate the Direction and Functional Strength between Neural Populations, vol. 9 32.

Park, J.W., Vahidi, B., Taylor, A.M., Rhee, S.W., Jeon, N.L., 2006. Microfluidic culture platform for neuroscience research. Nat. Protoc. 1 (4), 2128–2136.

Poli, D., Pastore, V.P., Massobrio, P., 2015. Functional Connectivity in in Vitro Neuronal

Assemblies, vol. 9 57.
Potter, S.M., DeMarse, T.B., 2001. A new approach to neural cell culture for long-term studies. J. Neurosci. Methods 110 (1), 17–24.
Sanhueza, M., Fernandez-Villalobos, G., Stein, I.S., Kasumova, G., Zhang, P., Bayer, K.U., et al., 2011. Role of the CaMKII/NMDA receptor complex in the maintenance of synaptic strength. J. Neurosci. : Off. J. Soc. Neurosci. 31 (25), 9170–9178.
Taylor, A.M., Dieterich, D.C., Ito, H.T., Kim, S.A., Schuman, E.M., 2010. Microfluidic local perfusion chambers for the visualization and manipulation of synapses. Neuron 66 (1), 57–68.
Toivanen, M., Pelkonen, A., Mäkinen, M., Ylä-Outinen, L., Sukki, L., Kallio, P., et al., 2017. Optimised PDMS Tunnel Devices on MEAs Increase the Probability of Detecting Electrical Activity from Human Stem Cell-Derived Neuronal Networks, vol. 11 606.
Tong, Z., Segura-Feliu, M., Seira, O., Homs-Corbera, A., Del Río, J.A., Samitier, J., 2015. A microfluidic neuronal platform for neuron axotomy and controlled regenerative studies. RSC Adv. 5 (90), 73457–73466.
Tsantoulas, C., Farmer, C., Machado, P., Baba, K., McMahon, S.B., Raouf, R., 2013. Probing functional properties of nociceptive axons using a microfluidic culture system. PLoS One 8 (11), e80722.
van de Wijdeven, R., Ramstad, O.H., Bauer, U.S., Halaas, Ø., Sandvig, A., Sandvig, I.J.B.M., 2018. Structuring a Multi-Nodal Neural Network in Vitro within a Novel Design Microfluidic Chip, vol. 20. pp. 9 1.
Virlogeux, A., Moutaux, E., Christaller, W., Genoux, A., Bruyère, J., Fino, E., et al., 2018. Reconstituting corticostriatal network on-a-Chip reveals the contribution of the presynaptic compartment to huntington's disease. Cell Rep. 22 (1), 110–122.
Wang, Y., Balaji, V., Kaniyappan, S., Krüger, L., Irsen, S., Tepper, K., et al., 2017. The release and trans-synaptic transmission of Tau via exosomes. Mol. Neurodegener. 12, 5.
Yap, Y.C., Dickson, T.C., King, A.E., Breadmore, M.C., Guijt, R.M., 2014. Microfluidic culture platform for studying neuronal response to mild to very mild axonal stretch injury. Biomicrofluidics 8 (4) 044110.